

Hybridization of Photoactive Titania Nanoparticles with Mesoporous Silica Nanoparticles and Investigation of Their Photocatalytic Activity

Norihiro Suzuki,[1] Xiangfen Jiang,[1,2] Logudurai Radhakrishnan,[1] Kimiko Takai,[1] Kotaro Shimasaki,[3] Yu-Tzu Huang,[4] Nobuyoshi Miyamoto,*[3] and Yusuke Yamauchi*[1,2,5]

[1]World Premier International (WPI) Research Center for Materials Nanoarchitectonics (MANA), National Institute for Materials Science (NIMS), 1-1 Namiki, Tsukuba, Ibaraki 305-0044

[2]Faculty of Science and Engineering, Waseda University, 3-4-1 Okubo, Shinjuku-ku, Tokyo 169-8555

[3]Department of Life, Environment and Materials Science, Faculty of Engineering, Fukuoka Institute of Technology (FIT), 3-30-1 Wajiro-Higashi, Higashi-ku, Fukuoka 811-0295

[4]Department of Bioenvironmental Engineering and R&D Center for Membrane Technology, Chung Yuan Christian University, No. 200, Chung Pei Road, Chung Li 320, Taiwan

[5]Precursory Research for Embryonic Science and Technology (PRESTO), Japan Science and Technology Agency (JST), 2-1 Hirosawa, Wako, Saitama 351-0198

Received January 27, 2011; E-mail: miyamoto@fit.ac.jp, Yamauchi.Yusuke@nims.go.jp

Here we demonstrate that photoactive titania (titanium dioxide) nanoparticles are successfully hybridized with an optimized amount of mesoporous silica (silicon dioxide) nanoparticles to realize drastic improvement of photocatalitic activity of the titania nanoparticles. Various types of mesoporous silica/titania composites are prepared by changing the amounts of doped mesoporous silica. Low-angle XRD patterns and N_2 adsorption–desorption isotherms reveal that the original mesostructures and pore sizes of mesoporous silica nanoparticles are well maintained even after hybridization with the titania nanoparticles. From SEM and TEM observation, it is confirmed that both the nanoparticles are homogeneously dispersed in the composite matrix. The obtained mesoporous silica/titania composites show excellent photocatalytic activity in the decomposition of methylene blue (MB), in comparison with titania nanoparticles without mesoporous silica. By hybridization with mesoporous silica, the photogenerated radicals from titania surfaces can efficiently react with many MB molecules captured inside the mesopores.

Among functional inorganic materials, titania (TiO_2) has currently received much attention owing to its prevalent applications in various fields such as photocatalysts, solar energy converters, and electrochromic devices.[1–10] Photocatalytic application using titania materials is one of the most focused applications worldwide. Numerous organic pollutants present in air or water can be easily decomposed by photocatalysts.[11] Surface area, crystal size, and crystallinity in the titania particles strongly influence their photocatalytic activity.[12] Nanocrystalline titania is a wide gap semiconductor which shows photocatalytic activity by absorbing UV light. Recently, there have been several reports on the synthesis of titania materials with enhanced activity.[13,14]

From the viewpoint of practical applications, fabrication of titania on an industrial scale is significant. For better utilization of solar energy, it is also desired to enhance the photocatalytic properties. In previous reports, titania particles with hierarchically porous structures show good photocatalytic properties owing to their high surface area.[14,15] However, as crystallization proceeds from amorphous material, the mesostructure collapses and the decrease of active surface area reduces the photocatalytic activity.[16] An alternative way to enhance the photocatalytic activity is the hybridization of titania with nanostructured silica.[17–22] The strong adsorption ability of dye molecules to the silica surface gives rise to notable reinforced interactions between the dye molecules and photocatalyst surface, leading to improved photocatalytic activity. Although several reports have appeared, the utilized silica nanoparticles had no porosity in many cases and those materials did not possess high surface area, resulting in low photocatalytic efficiency. Deposition of titania nanoparticles inside the pores of mesoporous silicas has also been attempted by post-treatment, however the controlled deposition of the desired amount of titania nanoparticles uniformly is still to be investigated.[23–26] Doping of titanium species into the mesoporous silica framework is also conducted,[27,28] though the controlling of co-condensation of titanium and silicon alkoxides is complex and the collapse of the mesostructure after calcination is still troublesome. Due to these drawbacks, low cost and large-scale production of the materials on an industrial scale is prevented. Anatase/silica composites with high surface area have been also fabricated in an attempt to enhance the adsorption ability of the solid catalysts.[29–35] However their photocatalytic activity is less than commercially available titania nanoparticles (Degussa P-25), even though the adsorption properties are improved in most cases.

Published on the web June 25, 2011; doi:10.1246/bcsj.20110027

Table 1. Physicochemical Properties of Synthesized Silica/Titania Nanocomposite Photocatalysts

Sample	Pore–pore distance[a] /nm	BET surface area[b] /$m^2\,g^{-1}$	Total pore volume[b] /$cm^3\,g^{-1}$	Average pore size[b] /nm	Adsorbed MB[c] /mmol g^{-1}-catalyst	Adsorbed MB[c] /mmol g^{-1}-TiO_2	Initial reaction rate[d] /min^{-1}
SiO_2_0	—	32.85	0.049	—	0.041	0.041	0.071
SiO_2_20	4.7	231.88	0.281	2.9	0.112	0.140	0.103
SiO_2_40	5.2	365.79	0.424	2.8	0.121	0.202	0.117
SiO_2_60	5.0	508.53	0.588	2.8	0.132	0.331	0.144
SiO_2_80	5.0	569.38	0.639	2.7	0.142	0.711	0.032
SiO_2_100	5.0	656.46	0.724	2.4	0.145	—	—

a) Pore-to-pore distances were calculated from low-angle XRD diffraction patterns. b) The BET surface areas, total pore volumes, and average mesopore sizes were calculated from the N_2 adsorption–desorption isotherms. c) The amounts of methylene blue (MB) adsorbed photocatalysts were estimated from the change of absorbance in visible spectra. d) Initial reaction rates were estimated from the change in the natural logarithm of $[MB]/[MB]_0$ with the reaction times.

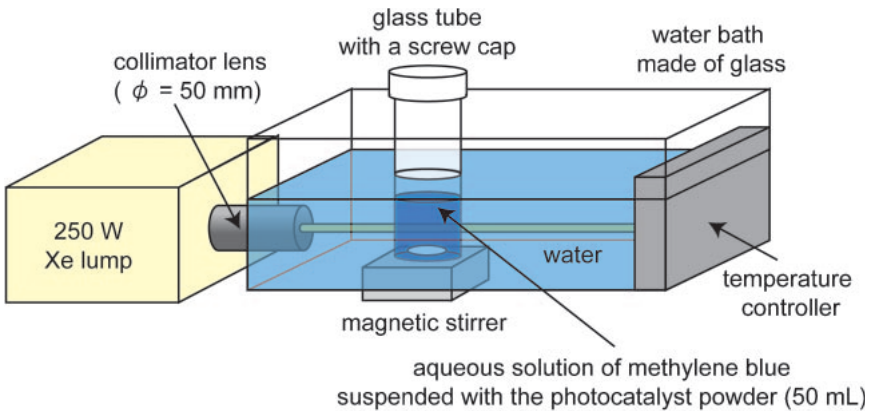

Scheme 1. Experimental apparatus for photocatalytic test.

In this paper, we report smart hybridization of photoactive titania nanoparticles with mesoporous silica nanoparticles. Since the particle size of mesoporous silica was almost identical to that of titania, both the nanoparticles could be homogeneously mixed in the composites. The prepared mesoporous silica/titania composites showed enhanced photocatalytic activity as well as higher adsorption capacity, in comparison with unmodified titania nanoparticles. Although there have been a few reports on the evaluation of adsorption and photocatalytic activity on nanostructured silica/titania composites, the actual role of the mesoporous silica has not been clarified yet. Here, we carefully investigated adsorption and photocatalytic activity to understand the real role of mesoporous silica, by using various composites with different amounts of mesoporous silica.

Experimental

Materials. Titania nanoparticles (Product name: P25) were obtained from Degussa, Japan Co. Tetraethyl silicate (Tetraethylorthosilicate, TEOS), hydrochloric acid, and ethanol (99.5%) were purchased from Nacalai Tesque, Inc. A triblock copolymer Pluronic F127 was acquired from Aldrich. Methylene blue (MB) was purchased from Waldeck GmbH & Co KG. All chemicals were used without further purification.

Synthesis of Silica/Titania Nanoparticle Composite. According to the previous papers, mesoporous silica nanoparticle with 20–30 nm diameter were prepared first (Figure S1).[36] Then, titania nanoparticles (P25) were added to the suspension of mesoporous silica nanoparticles and mixed thoroughly by ultrasonication for 20 min. After that, the mixtures were put on a plastic dish and the solvent was evaporated completely. The size of the utilized mesoporous silica nanoparticle was almost the same as that of the titania nanoparticles (Figure S1). Finally, the obtained powders were calcined at 650 °C for 6 h in air. Various mesoporous silica/titania composites with different amounts of mesoporous silica were prepared. The total weight of the composites was fixed to 0.5 g and the weight ratios of mesoporous silica to titania were gradually changed from 0 to 100 wt %. Hereafter, mesoporous silica/titania composites were abbreviated as **SiO_2_*x*** where ***x*** indicated the weight ratios of mesoporous silica in the final composites.

Investigation of Photocatalytic Activity. Each photocatalyst powder (0.01 g) was dispersed in 50 mL of MB aqueous solutions (0.03 mM) in a glass tube with 4.0 cm in a diameter, followed by ultrasonication for 30 s. The mixture was stirred for 60 min in dark (the adsorption process) and irradiated for up to 30 min (photolysis) with stirring; the collimated light from a 250 W Xe-lump (USHIO, UI-501C) was irradiated without any optical filter to the sample in the glass tube fixed in the temperature-controlled water bath (30 °C) (Scheme 1). While the glass tube was capped to avoid

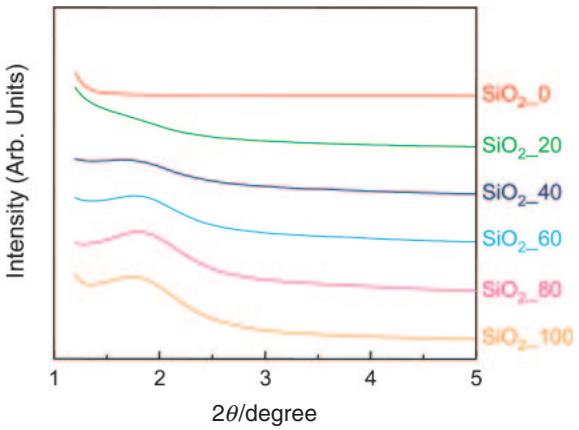

Figure 1. Low-angle XRD patterns of mesoporous silica/titania composites with different amounts of mesoporous silica.

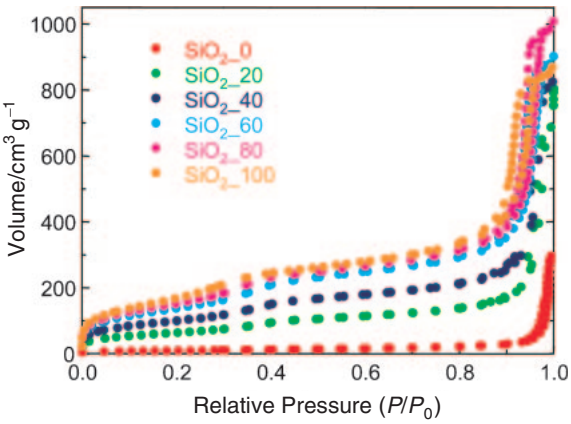

Figure 2. N_2 adsorption–desorption isotherms of mesoporous silica/titania composites with different amounts of mesoporous silica.

evaporation of the solvent during adsorption and photolysis, ca. 3 mL of the solution was sampled several times by opening the cap. The sampled solutions were filtered with a syringe driven poly(tetrafluoroethylene) (PTFE) filter (Millex SLLGH04NL with pore size of 0.20 μm) and measured with a UV–vis spectrophotometer (Shimadzu, UV-3100PC). The photolysis was conducted in open air, the liquid in the tube was always in contact with the air in the upper part of the vessel (ca. 110 mL), and the capped vessel was often opened for sampling. The spectroscopic measurement was also conducted by using an open cell. Since all the experiments were conducted by using a common setup and conditions, we can quantitatively compare the adsorption and photocatalytic properties of the samples presented here.

Characterization. Low-angle XRD patterns were measured on a Rigaku RINT 2000/PC (Cu Kα). During the measurement, the scanning rate was $1° \text{ min}^{-1}$. N_2 adsorption–desorption isotherms were measured with BELSORP-mini II (BEL JAPAN) at 77 K. Before the measurement, the samples were degassed under vacuum at 100 °C for 24 h with BELPREP-vac II (BEL JAPAN). The morphology of the composites was observed with a HITACHI S-4800 field emissive scanning electron microscopy (FE-SEM). Transmission electron microscopic (TEM) images were taken by using JEOL JEM-2010 operated at the accelerating voltage of the electron beam 200 kV. For the observation of TEM images, the powder samples were sonicated in ethanol and mounted and dried naturally onto Cu microgrids.

Results and Discussion

The fabricated mesoporous silica/titania composites were characterized by low-angle XRD measurement, N_2 adsorption–desorption isotherms, and SEM and TEM observation. Figure 1 shows the XRD patterns for all of the composites. The XRD pattern for **SiO_2_100** showed a peak at $2\theta = 1.8°$, revealing mesostructural ordering. The calculated pore-to-pore distance was estimated to be 5.0 nm, which coincided with the value estimated by TEM image. For all of the composites except **SiO_2_0**, XRD patterns of each composite possessed a single peak appearing at nearly the same diffraction angle. With the decrease of mesoporous silica amounts, however, the intensities of the peaks gradually decreased. The N_2 adsorption–desorption isotherms of the composites are displayed in Figure 2. A typical type IV isotherm was clearly confirmed. The increase of the adsorbed gas volume at the lower relative pressure indicated the presence of uniform mesopores (with pore diameter of around 3 nm). The BET surface areas and the total pore volumes calculated from the absorption brunch are listed in Table 1. With increase of the mesoporous silica amounts, both BET surface area and total pore volume increased, while the average pore diameter was almost identical. These above data clarified that the original mesoporosity of the mesoporous silica nanoparticles were well maintained even after the composite fabrication.

To further understand how mesoporous silica nanoparticle and titania nanoparticles were assembled in the composites, SEM and TEM observations were conducted (Figure 3). From SEM images (Figures 3a and 3b), it was seen that the 20–30 nm spherical nanoparticles were aggregated in the composites. TEM images (Figures 3c–3f) clearly revealed that both mesoporous silica nanoparticles and titania nanoparticles were dispersed homogeneously in the composites. Also, several void spaces was observed among the aggregated nanoparticles, providing high accessibility of guest molecules from outside particles.

The adsorption and photocatalytic properties of the obtained mesoporous silica/titania composites were examined by dispersing the catalyst powders in an aqueous solution of MB (0.03 M). Figure 4 shows the time course of the visible spectra of the MB solution, which are sampled and filtrated from the dispersion, during the adsorption and photolysis of MB. Before light irradiation (0–60 min), the absorbance of the peak at 664 nm ascribable to MB decreased rapidly, indicating the adsorption of MB to the catalysts (Figure 4a). After beginning light irradiation (60–90 min), the absorbance began to decrease again, accompanied by blue shift of the wavelengths of the absorption maxima (Figures 4b–4f). The decrease of peak intensity accompanying the blue shift was due to the photocatalytic decomposition of MB molecules.[32] In contrast, when **SiO_2_100** (i.e., pure mesoporous silica) was used under the same

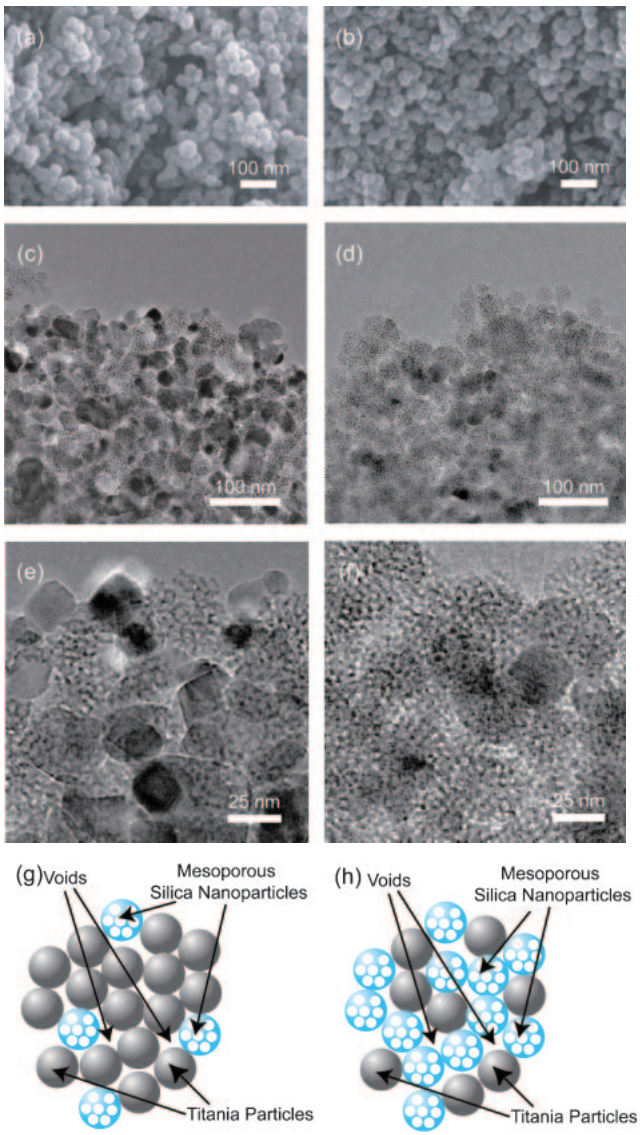

Figure 3. (a, b) SEM and (c–f) TEM images of mesoporous silica/titania composites with different amounts of mesoporous silica ((a, c, e, and g) **SiO_2_20**, (b, d, f, and h) **SiO_2_60**). Figures (g) and (h) show schematic illustration of the obtained composites.

reaction conditions, the decrease of peak intensity and similar peak shift was not observed at all. As shown in Figures 4b–4f, the continuous decrease of peak intensity strongly suggested that the MB and the compounds formed by partial decomposition of MB were not fixed in the mesopores, but they were in the adsorption equilibrium during the photolysis.

Figure 5 shows the time course of the absorbance at the wavelength of absorption maxima observed in the visible spectra. In all the systems, adsorption of MB reached equilibrium within 60 min. The total amounts of adsorbed MB at the equilibrium were listed in Table 1. The larger amounts of MB were adsorbed as the weight ratios of mesoporous silica nanoparticles increased. After beginning the light irradiation, the absorbance further decreased due to decomposition of MB molecules. After 60 min of UV irradiation, all the MB molecules were completely decomposed in the system of mesoporous silica/titania composites, while unreacted MB molecules still remained in the titania nanoparticle system (**SiO_2_0**). According to the Langmuir–Hinshelwood model,[18] the photocatalytic reaction proceeds in first-order kinetics at the limit of very low reactant concentration. To evaluate the kinetics of the photolysis on this model, we plotted the natural logarithm of the $[MB]/[MB]_0$, where $[MB]_0$ is the value at the absorption equilibrium, as the function of photoirradiation time (see inset in Figure 5). The present system basically obeyed this model at the beginning of the reaction. The initial reaction rate for 6 min after light irradiation is summarized in Table 1. Except **SiO_2_80**, the reaction rates were improved by hybridization with mesoporous silica nanoparticles, despite the fact that the amounts of photoactive titania nanoparticles embedded in the catalysts decreased.

It should be importantly noted that the initial reaction rates were proportional to the total amounts of MB molecules accommodated in the photocatalysts (Table 1). In the present MB decomposition process, lots of radicals are generated on the anatase surface at the initial stage of UV irradiation. Then, a lot of hydroxyl radicals (•OH) attack the MB molecules, initiating the photocatalytic degradation through hydrogen abstraction from methyl groups. The hydrogen abstraction produces the $\bullet CH_2$ radical, which can be further attacked by either O_2 or O_2^-, resulting in demethylation.[37]

The most important point is that the generated hydroxyl radicals effectively attack the MB molecules. As mentioned above, by the hybridization with mesoporous silica with high surface area, a large number of the MB molecules were captured near the active titania surface. Therefore, the hydroxyl radicals generated from photocatalytically active sites can easily transport many MB molecules, thereby leading to the acceleration of reaction rates for their decomposition. However, when the amount of mesoporous silica in the composite was very high (**SiO_2_80**), the initial reaction rate decreased dramatically. In general, the radicals are very unstable and the recombination of the photogenerated radicals frequently occurs. When the mesoporous silica amount becomes high, the distance between neighboring titania nanoparticles tends to increase. Then, the radicals cannot reach all the MB molecules, resulting in the slowest initial reaction rate. Among the composites with various amounts of mesoporous silica, **SiO_2_60** exhibited the fastest initial reaction rate.

In the present study, it is notable that both adsorption capability and photocatalytic activity were improved by hybridization with the nanoporous silica nanoparticles. It has been generally known that the adsorption capability is improved by hybridization with porous materials.[29–35] This is also the case for the present systems and rationalized by increase in the BET surface area. However, in most of the previous cases,[29–35] the enhancement of the photocatalytic activity by the hybridization with nanoporous silica could not be confirmed clearly, because nanoporous silica/titania composites have not been directly compared with unmodified titania nanoparticles themselves.[29–35] Furthermore, in some previous cases, the photocatalytic activity was reduced in comparison with unmodified titania nanoparticles, even though the initial adsorption capability increased.[34]

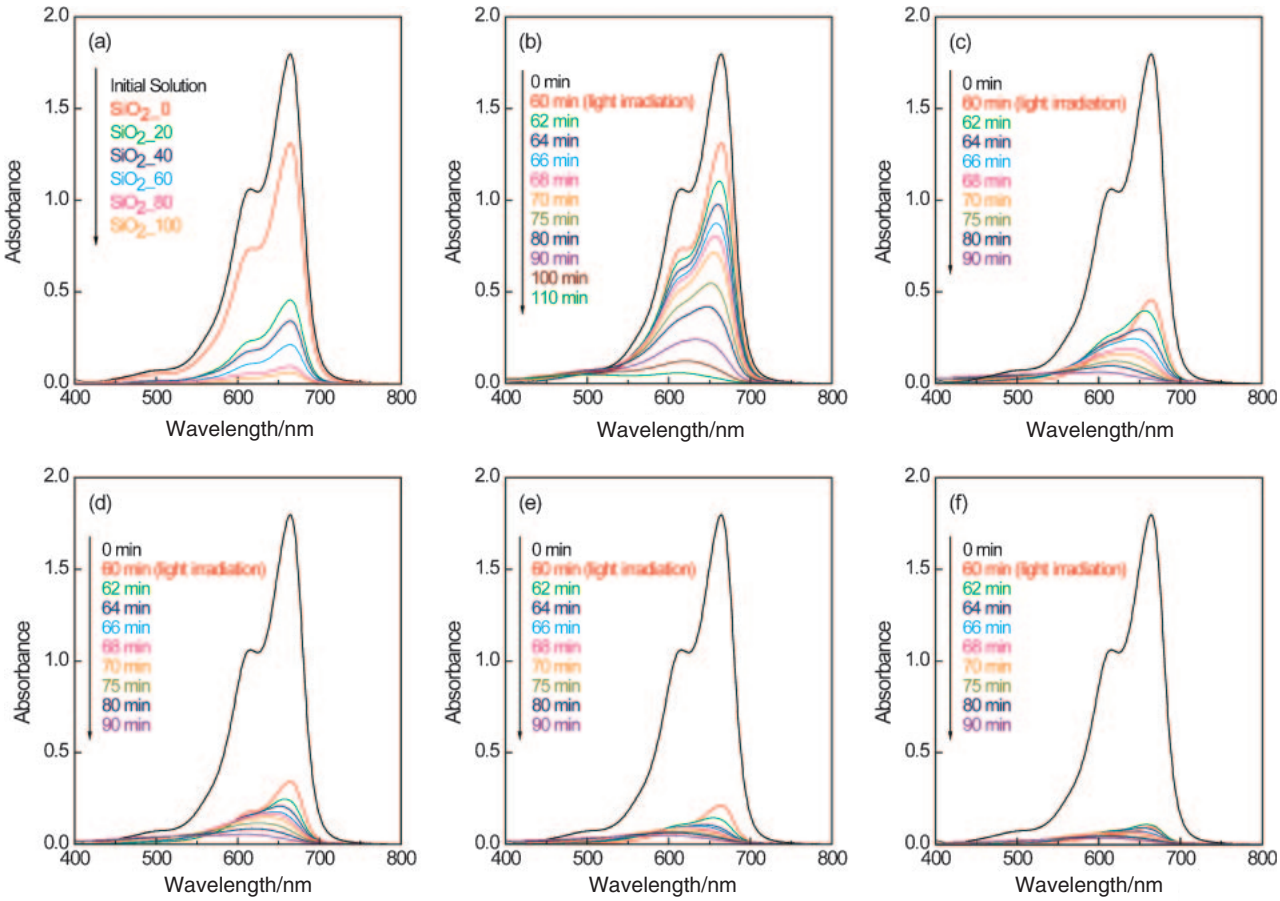

Figure 4. (a) Visible spectra of the initial aqueous MB solution and the filtered solutions sampled from aqueous MB/photocatalyst mixtures after saturation in the dark. (b–f) Visible spectra of the filtered solutions sampled from aqueous MB/photocatalyst mixtures during photolysis experiments. Used photocatalyst are (b) **SiO_2_0**, (c) **SiO_2_20**, (d) **SiO_2_40**, (e) **SiO_2_60**, and (f) **SiO_2_80**, respectively.

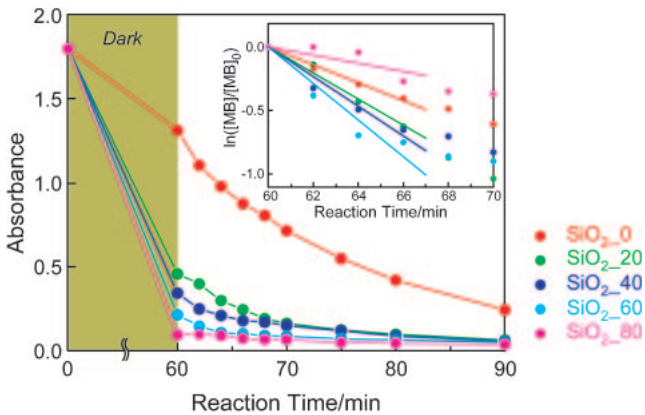

Figure 5. The time course of the absorbance (at the wavelength of the absorption maximum) observed by visible spectra of the filtered solutions sampled from aqueous MB/photocatalyst mixtures during the adsorption and photolysis experiments. The inset shows the kinetics of photolysis of MB in the presence of photocatalyst. The natural logarithm of $[MB]/[MB]_0$ is plotted versus photo-irradiation time, where [MB] is the concentration of MB remaining in the solution and $[MB]_0$ is [MB] at adsorption equilibrium. Linear regression lines for calculation of the initial reaction rate are also included.

As revealed by visible spectra (Figures 4b–4f), the MB molecules could quickly diffuse from solution phase to the photoactive titania sites and the compounds formed by the photolysis could also quickly diffuse from the reaction site to outside of the particles, which may be helped by rather loose adsorption of the compounds to the catalyst. Such rapid diffusion of both MB molecules and the compounds formed by the photolysis is helpful for accelerating the decomposition of MB molecules. The pore size of the mesoporous silica covering titania surface is around 3 nm (Table 1), which is enough for rapid diffusion of MB molecules ($1.6\,\text{nm} \times 0.7\,\text{nm} = 1.1\,\text{nm}^2$) and the compounds. In the previous investigation on diffusion rate of organic molecules in microporous silica films, it was shown that the organic molecules could be immediately dispersed to 50 nm depth in the films.[31] In the present system, the particle sizes of mesoporous silica were around 30 and 40 nm (Figures 3e and 3f) which can allow for rapid diffusion of MB molecules and the compounds through the whole silica particle. The presence of the voids among the assembled nanoparticles (Figures 3e and 3f) also nicely assists the rapid diffusion.

Through the above photocatalytic tests using the various composites with different amounts of mesoporous silica, we could find out the optimized silica amounts for rapid photo-

decomposition reaction of MB molecules. As discussed above, the effective adsorption capacity plays an important role for acceleration of reaction rate. As the amounts of the doped mesoporous silica particles in composites were increased, the total adsorption capacity of organic molecules was also increased, however gradually the radicals photogenerated on titania nanoparticles could not effectively reach the MB molecules captured inside the mesopores.

Conclusion

We successfully demonstrated smart design of mesoporous silica/titania composites as photocatalysts. Through the quantitative understanding of adsorption capability and decomposition rate of MB molecules, the importance of hybridization with mesoporous silica was clarified for the first time. The effective adsorption capacity of MB molecules into the photocatalysts is necessary. With increasing the weight ratio of mesoporous silica, the amount of adsorbed MB molecules per titania particles also increased due to the larger surface area. Because of this, initial reaction rate of silica/titania nanocomposite photocatalysts was faster than that of nonporous titania (**SiO_2_0**), though **SiO_2_80** was an exception. Very recently, the precise structural control of spherical mesoporous silica nanoparticles has become an important topic in biomaterials research, due to high biocompatibility.[38–45] The present paper shows significance for use of mesoporous silica nanoparticles to realize high photocatalytic performance, which opens the door for new application using mesoporous silica nanoparticles. In the future, by further controlling particle sizes and mesopore sizes precisely, we can expect enhanced photocatalytic properties.

Supporting Information

Figure S1: SEM images of original mesoporous silica nanoparticles and titania nanoparticles (P25). This material is available free of charge on the web at http://www.csj.jp/journals/bcsj/.

References

1 A. Fujishima, K. Honda, *Nature* **1972**, *238*, 37.
2 *Solid State Gas Sensors*, ed. by P. T. Moseley, B. C. Tofield, IOP Publishing Ltd., Bristol, **1987**.
3 B. O'Regan, M. Grätzel, *Nature* **1991**, *353*, 737.
4 Y. Ma, J. Yao, *J. Photochem. Photobiol., A* **1998**, *116*, 167.
5 D. Beydoun, R. Amal, G. K.-C. Low, S. McEvoy, *J. Phys. Chem. B* **2000**, *104*, 4387.
6 M. Grätzel, *Nature* **2001**, *414*, 338.
7 S. Si, K. Huang, X. Wang, M. Huang, H. Chen, *Thin Solid Films* **2002**, *422*, 205.
8 U. Diebold, *Surf. Sci. Rep.* **2003**, *48*, 53.
9 A. Nakajima, H. Obata, Y. Kameshima, K. Okada, *Catal. Commun.* **2005**, *6*, 716.
10 X. Chen, S. S. Mao, *Chem. Rev.* **2007**, *107*, 2891.
11 M. Stylidi, D. I. Kondarides, X. E. Verykios, *Appl. Catal., B* **2003**, *40*, 271.
12 A. Hagfeldt, M. Grätzel, *Chem. Rev.* **1995**, *95*, 49.
13 C. Aprile, A. Corma, H. Garcia, *Phys. Chem. Chem. Phys.* **2008**, *10*, 769.
14 F. Iskandar, A. B. D. Nandiyanto, K. M. Yun, C. J. Hogan, Jr., K. Okuyama, P. Biswas, *Adv. Mater.* **2007**, *19*, 1408.
15 T. Kimura, N. Miyamoto, X. Meng, T. Ohji, K. Kato, *Chem.—Asian J.* **2009**, *4*, 1486.
16 H. Shibata, T. Ogura, T. Mukai, T. Ohkubo, H. Sakai, M. Abe, *J. Am. Chem. Soc.* **2005**, *127*, 16396.
17 C. Anderson, A. J. Bard, *J. Phys. Chem.* **1995**, *99*, 9882.
18 C. Anderson, A. J. Bard, *J. Phys. Chem. B* **1997**, *101*, 2611.
19 M. Hirano, K. Ota, *J. Am. Ceram. Soc.* **2004**, *87*, 1567.
20 C. M. Whang, Y. K. Kim, J. G. Kim, W. I. Lee, Y. H. Kim, *Mater. Sci. Forum* **2004**, *449–452*, 1117.
21 M. Fujimoto, T. Ohno, H. Suzuki, H. Koyama, J. Tanaka, *J. Am. Ceram. Soc.* **2005**, *88*, 3264.
22 Z. Li, B. Hou, Y. Xu, D. Wu, Y. Sun, *J. Collolid Interface Sci.* **2005**, *288*, 149.
23 S. Perathoner, P. Lanzafame, R. Passalacqua, G. Centi, R. Schlögl, D. S. Su, *Microporous Mesoporous Mater.* **2006**, *90*, 347.
24 X. Wang, W. Lian, X. Fu, J.-M. Basset, F. Lefebvre, *J. Catal.* **2006**, *238*, 13.
25 W. Wang, M. Song, *Microporous Mesoporous Mater.* **2006**, *96*, 255.
26 E. Beyers, E. Biermans, S. Ribbens, K. De Witte, M. Mertens, V. Meynen, S. Bals, G. Van Tendeloo, E. F. Vansant, P. Cool, *Appl. Catal., B* **2009**, *88*, 515.
27 Z. Zhu, M. Hartmann, E. M. Maes, R. S. Czernuszewicz, L. Kevan, *J. Phys. Chem. B* **2000**, *104*, 4690.
28 K. De Witte, A. M. Busuioc, V. Meynen, M. Mertens, N. Bilba, G. Van Tendeloo, P. Cool, E. F. Vansant, *Microporous Mesoporous Mater.* **2008**, *110*, 100.
29 T. Kasahara, K. Inumaru, S. Yamanaka, *Microporous Mesoporous Mater.* **2004**, *76*, 123.
30 K. Inumaru, T. Kasahara, M. Yasui, S. Yamanaka, *Chem. Commun.* **2005**, 2131.
31 E. Allain, S. Besson, C. Durand, M. Moreau, T. Gacoin, J.-P. Boilot, *Adv. Funct. Mater.* **2007**, *17*, 549.
32 X. Li, J. Ye, *J. Phys. Chem. C* **2007**, *111*, 13109.
33 M. Takeuchi, T. Kimura, M. Hidaka, D. Rakhmawaty, M. Anpo, *J. Catal.* **2007**, *246*, 235.
34 R. Kato, N. Shimura, M. Ogawa, *Chem. Lett.* **2008**, *37*, 76.
35 Y. Shiraishi, Y. Sugano, D. Inoue, T. Hirai, *J. Catal.* **2009**, *264*, 175.
36 V. Cauda, A. Schlossbauer, J. Kecht, A. Zürner, T. Bein, *J. Am. Chem. Soc.* **2009**, *131*, 11361.
37 Z. Yu, S. S. C. Chuang, *J. Phys. Chem. C* **2007**, *111*, 13813.
38 T.-W. Kim, P.-W. Chung, V. S.-Y. Lin, *Chem. Mater.* **2010**, *22*, 5093.
39 C. E. Fowler, D. Khushalani, B. Lebeau, S. Mann, *Adv. Mater.* **2001**, *13*, 649.
40 S. Giri, B. G. Trewyn, V. S. Y. Lin, *Nanomedicine* **2007**, *2*, 99.
41 T.-W. Kim, P.-W. Chung, I. I. Slowing, M. Tsunoda, E. S. Yeung, V. S.-Y. Lin, *Nano Lett.* **2008**, *8*, 3724.
42 I. I. Slowing, C.-W. Wu, J. L. Vivero-Escoto, V. S.-Y. Lin, *Small* **2009**, *5*, 57.
43 J. Lu, M. Liong, Z. Li, J. I. Zink, F. Tamanoi, *Small* **2010**, *6*, 1794.
44 Y. Hoshikawa, H. Yabe, A. Nomura, T. Yamaki, A. Shimojima, T. Okubo, *Chem. Mater.* **2010**, *22*, 12.
45 J. Gu, W. Fan, A. Shimojima, T. Okubo, *Small* **2007**, *3*, 1740.